Sensors and Actuators A 178 (2012) 26–31

Contents lists available at SciVerse ScienceDirect

Sensors and Actuators A: Physical

journal homepage: www.elsevier.com/locate/sna

ZnO nanorods grown on polymer substrates as UV photodetectors

I-Chuan Yao [a], Tseung-Yuen Tseng [b,*], Pang Lin [a]

[a] Department of Materials Science and Engineering, National Chiao Tung University, Hsinchu 300, Taiwan
[b] Department of Electronics Engineering and Institute of Electronics, National Chiao Tung University, Hsinchu 300, Taiwan

ARTICLE INFO

Article history:
Received 23 September 2011
Received in revised form 27 January 2012
Accepted 31 January 2012
Available online 11 February 2012

Keywords:
Zinc oxide nanorod
Photodetector
Polymer substrate
High reliability

ABSTRACT

Vertical well-aligned and uniform ZnO nanorods were successfully prepared on low cost and flexible PET polymer substrate by aqueous solution method under various growth conditions. Current–voltage (I–V) and current–time (I–t) relationships measurements demonstrate that the photocurrent can be increased by more than 25 times upon UV illumination (λ = 365 nm) with a power density of 70 μW/cm^2. The photocurrents can be repeatedly and reproducibly switched by modulating UV exposure with power densities of 25–70 μW/cm^2. The fast response time (100 s) and rapid recovery time (120 s) are achieved in UV turn-on/off switching measurements. Owing to the good performance including mechanical flexibility, nondestructive properties, high reliability and multilevel photoresponse, the well-aligned ZnO nanorods grown on transparent and flexible PET polymer substrates have high potential for UV photodetector applications.

1. Introduction

One-dimensional (1D) zinc oxide (ZnO) nanomaterials have recently received much attention for their potential applications in field emitter [1,2], light emitting diode [3], chemical sensor [4] and photodetector [5–8]. Among various applications, ultraviolet (UV) photodetector is an important device that has a wide range of chemical and environmental detecting applications. Compared with the bulk or thin film photodetectors, the 1D nanostructures are able to provide higher sensitivity and faster response devices because they have larger aspect ratio of length to diameter and much higher surface area to volume ratio compared with their film and bulk materials counter parts [9]. The photodetector with high sensitive properties was prepared by aligned ZnO noanorods on paper substrates using low temperature chemical solution [10]. The colloidal ZnO nanoparticles on glass substrates formed by spin-coating were observed to have fast recovery time [11]. In addition, a simple wet chemical method combined with photolithography technique was used to prepare ZnO nanorods at selective areas, which exhibited a larger photoresponse than the thin film photosensors [12]. Obviously, the performances of the photodetectors were demonstrated to be improved through nanorod or nanoparticle form based on above mentioned previous results. Compared with Si, glass and paper substrates, the polyethylene terephthalate (PET) polymer substrates have the advantages of high transparency, good flexibility, and low cost [13]. Large area PET substrate is commercially available, which is a good substrate for the fabrication of flexible photodetectors. However, the photoresponsive properties of the nanorods grown on PET have received scarce attention. In this work, the vertically well-aligned ZnO nanorods are grown on ZnO buffer film/PET substrates using an aqueous solution method. The structure and morphology of ZnO nanorods and their UV photodetective properties are investigated.

2. Experimental

The schematic description of the ZnO nanorod photodetector is shown in Fig. 1. The fabrication of ZnO UV photodetectors is described as below. Before the ZnO nanorods are grown, a 10 nm-thick ZnO buffer layer is spin-coated onto PET substrate to reduce the mismatch between ZnO nanorods and polymer substrate. The two silver electrodes fabricated by E-gun evaporation with an area of 5 mm (W) × 15 mm (L) and thickness of about 48 nm are separated about 5 mm from each other. The silver electrodes have smooth surface based on the images of scanning electron microscope (not shown here). Unless specified, the aqueous synthesis of ZnO nanorods is carried out at 90 °C in a sealed kettle placed in a quartz beaker. The ZnO coated substrates are immersed in a precursor solution for 60, 30, 20 and 10 min, respectively. The precursor solution is prepared by mixing 0.25 M zinc chloride ($ZnCl_2$) with 7 ml ammonium hydroxide solution (NH_4OH). After the reaction, the substrates are removed from the solution, rinsed with deionized water, and dried in the air. ZnO-x is used to express the ZnO nanorods grown at different growth time, x. Surface morphologies and size distribution of the ZnO nanorods used in the photodetector fabrication are analyzed by field-emission scanning electron

* Corresponding author. Tel.: +886 3 5731879; fax: +886 3 5724361.
E-mail address: tseng@cc.nctu.edu.tw (T.-Y. Tseng).

0924-4247/$ – see front matter © 2012 Elsevier B.V. All rights reserved.
doi:10.1016/j.sna.2012.01.045

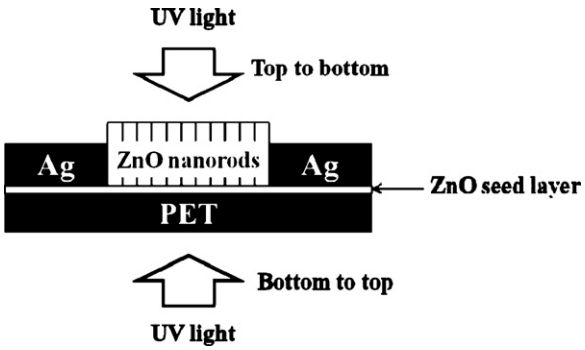

Fig. 1. Schematic diagram of ZnO nanorod photodetector.

microscope (FE-SEM, Hitachi S-4700I). X-ray diffraction (XRD, Bede D1), photoluminescence (PL) and transmission electron microscope (TEM, JEOL 2100F) observations are then utilized to characterize the crystallographic and optical properties of those ZnO nanorods. Both the current–voltage (I–V) characteristic and current–time (I–t) photoresponse are measured at room temperature in air under UV illumination at $\lambda = 365$ nm with power densities of 25, 35 and 70 $\mu W/cm^2$, respectively.

3. Results and discussion

Fig. 2(a)–(d) reveals the typical FE-SEM images of the ZnO nanorods synthesized for 60 and 10 min by the aqueous solution method. It can be observed the ZnO nanorods vertically well aligned grown on the ZnO film/PET substrate. The average length of ZnO nanorods decreases from 1520 ± 155.3 to 425 ± 25.3 nm and their average diameter decreases from 120 ± 22.3 to 30 ± 5.5 nm as the growth time decreased from 60 to 10 min. The ZnO nanorods with various growth times are uniformly grown on the ZnO film/PET substrates (Fig. 2(a)–(d)), indicating that the vertical nanorods with uniform length and diameter can be easily synthesized with the growth time of 10 min.

Fig. 3(a) indicates XRD patterns of ZnO nanorods with various growth times, exhibiting the single phase with wurtzite structure for all the nanorods. In addition, the intensity of (0 0 2) peak is much higher than those of other peaks, suggesting that the ZnO nanorods preferentially grow in the [0 0 1] direction. The intensity of (0 0 2) peak increases with an increase of the growth time, indicating that the crystallinity is improved by increasing growth time. Fig. 3(b) reveals the room temperature PL spectra of ZnO nanorods with a strong luminescence peak centered at around 377 nm, which represents the near-band-edge emission, while a weak broad band centered at around 550 nm is mainly attributed to oxygen vacancies existed in the ZnO crystals [14–16]. In addition, it also clearly indicates the blue shift of the UV peak position (from 377 to 374 nm) with reduced growth time. This phenomenon was explained that the decrease in the size of ZnO nanorods can induce the blueshift of the UV peak [17]. The inset of Fig. 3(b) shows the I_{UV}/I_{VIS} ratio as a function of growth time, where I_{UV} is the intensity of UV emission peak and I_{VIS} the intensity of visible emission peak. The I_{UV}/I_{VIS} ratio slightly increases with an increase of growth time, which has the same trend with the crystallinity improved by the increasing growth time (Fig. 3(a)). The bright field image of the ZnO-10 nanorods is shown in Fig. 4(a), revealing that the nanorod exhibits the diameter of the nanorod tip is slightly smaller than that of the bottom. The HRTEM image (inset at upper right corner of Fig. 4(a)) indicates that the nanorod is highly crystallized with a lattice spacing of 5.204 Å, which corresponds to the (0 0 2) plane in the ZnO crystal lattice. The selected area diffraction (SAED) pattern (inset at low left corner of Fig. 4(a)) identifies that the ZnO nanorod is grown along the [0 0 1] direction, which was confirmed with the result from XRD (Fig. 3(a)). The typical EDS spectrum for ZnO-10 nanorods shown in Fig. 4(b) indicates that the nanorods are composed of only Zn and O. The Cu and C signals originate from the TEM grid. No evidence of other impurities was found from the spectrum. With further quantitative analysis of EDS, it reveals that the atomic ratio of Zn/O is 43.3:56.7.

Taking advantage of the highly mechanical flexibility of the ZnO nanorods/PET substrate, ZnO-10 nanorods could be extremely bent

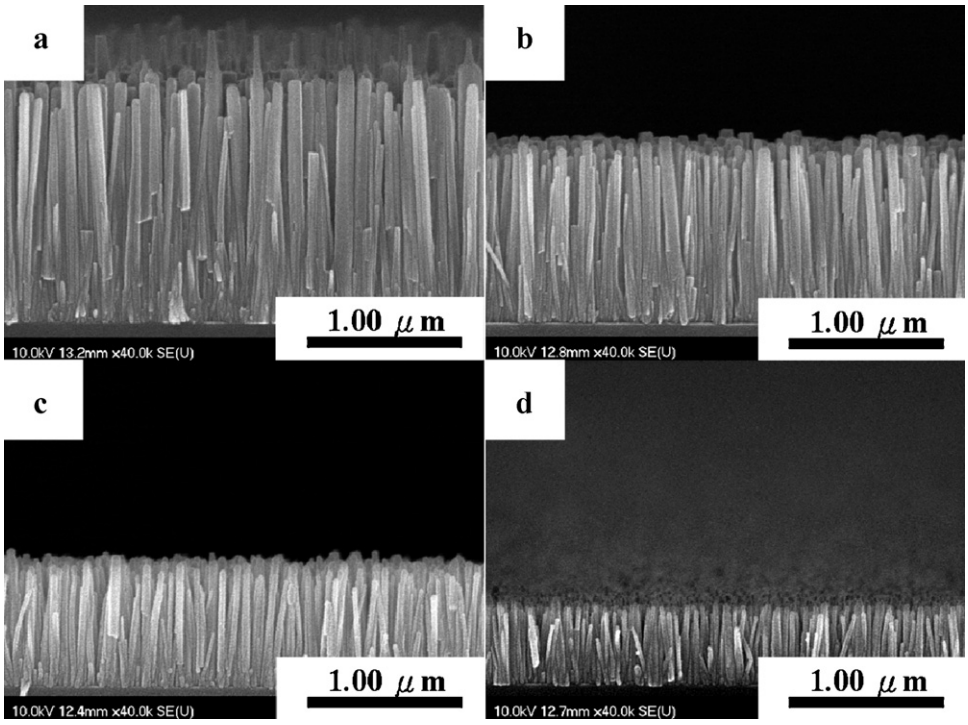

Fig. 2. Typical FE-SEM images of (a) ZnO-60, (b) ZnO-30, (c) ZnO-20 and (d) ZnO-10 nanorods, respectively.

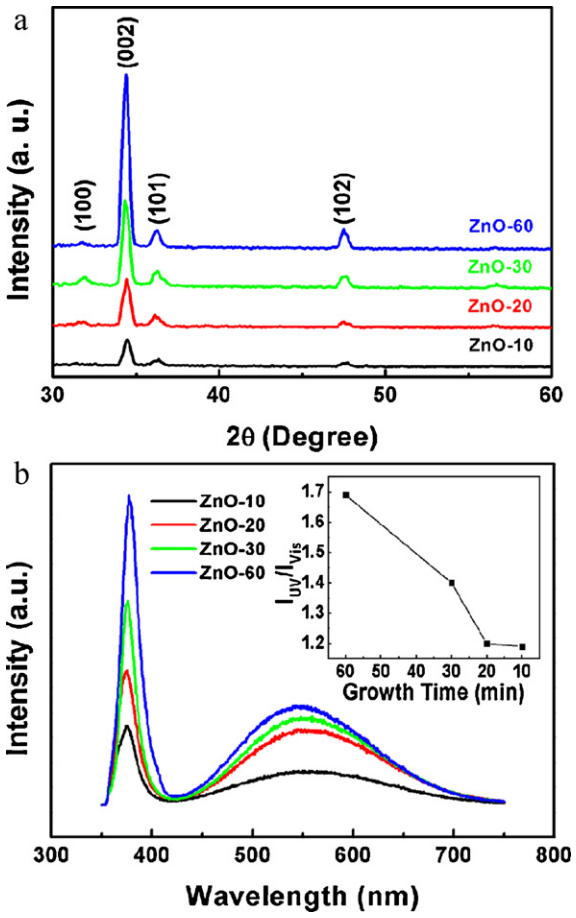

Fig. 3. (a) XRD patterns and (b) PL spectra of the ZnO nanorods with various growth times. Inset is the ratios of UV emission to visible light emission as a function of growth time.

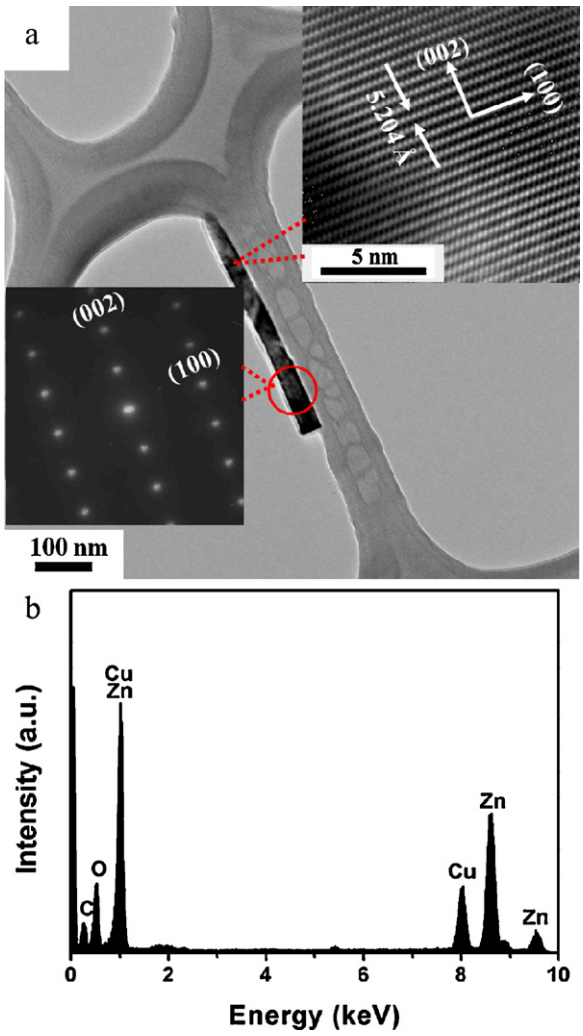

Fig. 4. (a) TEM bright image and (b) EDS analysis of the ZnO-10 nanorod. Inset is the SAED pattern and HRTEM image of the ZnO-10 nanorod.

without losing their structural integrity, as shown in Fig. 5(a)–(c). Despite the bending radius of 5 mm, the structural integrity was well maintained at convex and concave geometries. Fig. 5(d) depicts the current–voltage curves of ZnO-10 nanorods/PET substrate at the bending measurement. It is observed the typical Ohmic behavior and the currents of concave, flat and convex structures are 68.5, 63.2 and 61.3 nA at 0.5 V, respectively. The current variation between various structural geometries is negligible difference. It reveals good mechanical stability throughout the bending measurements.

Fig. 6(a) depicts *I–V* characteristics of the ZnO-10 nanorods photodetector measured in a dark environment and under illuminations by changing the DC bias from −5 to +5 V from bottom (the illumination underneath the polymer substrate) to top. During photocurrent measurement, the dark current is about 63.2 nA at a DC bias of 0.5 V. The small dark current is attributed to high resistance of the ZnO-10 nanorods. We are able to neglect the contact resistance between Ag and ZnO buffer layer and the resistance of the electrodes because the resistance of the Ag electrode (16.29 nΩ m at 18 °C) is much lower than that of the ZnO-10 nanorods [18]. With the same DC bias of 0.5 V, the measured currents are 0.66, 0.92 and 1.55 μA under 25, 35 and 70 μW/cm^2 UV light illuminations, respectively. The currents under 25, 35 and 70 μW/cm^2 UV illuminations are about 11,

Table 1
Comparisons of the performance of the ZnO photodetectors with various ZnO nanostructures.

Type of ZnO nanostructures	Substrate	Test UV intensity (μW/cm^2)	Response time (s)	Recovery time (s)	Reliability	Ref.
Nanoparticles (in O_2)	Silicon	20	≈10	≈50	4 cycles of switching	[23]
Nanotubes	Glass	–	≈130	≈250	4 cycles of switching	[24]
Single-microtube (in O_2)	–	21,700 at 50 cm distance	≈15	≈1850	4 cycles of switching	[25]
Nanowires	Glass	1000	40	55	–	[26]
Nanorods	Paper	–	≈800	≈600	5 cycles of switching	[10]
Nanorods	Glass	300	≈300	≈500	4 cycles of switching	[27]
Nanorods	Silicon	16	≈100	≈150	12 cycles of switching	[28]
In our work (ZnO-10/PET)	PET	25 35 70	100	120	1. 20 cycles of switching 2. Two-fold symmetry characteristic 3. Retention test (1, 50 and 100 h) 4. Multilevel photoresponse	

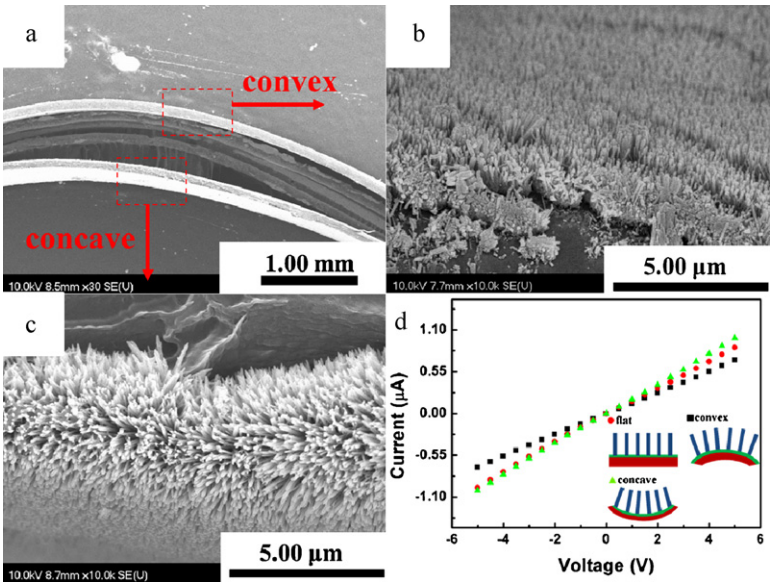

Fig. 5. (a) Low magnification SEM image of high bent ZnO-10/PET structure, (b) convex and (c) concave geometric side views and (d) *I–V* characteristics measured at different bending morphologies.

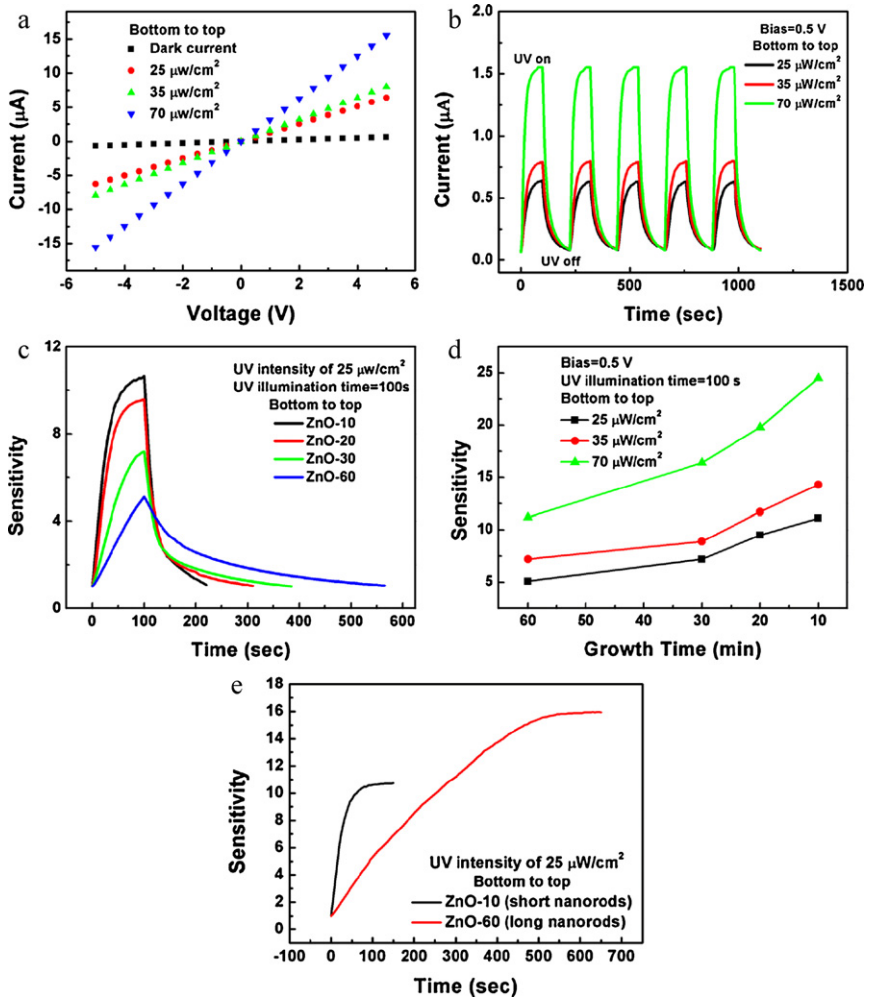

Fig. 6. UV photodetective properties: (a) *I–V* plot of ZnO-10 nanorods in the dark environment and under UV illumination (365 nm) with power densities of 25, 35 and 70 µW/cm^2, respectively. (b) Reversible switching properties of ZnO-10 nanorods. (c) Sensitivity vs time plots under 100 s illuminations of ZnO nanorods grown with various times at a power density of 25 µW/cm^2. (d) Sensitivity vs growth time curves of the nanorods at 0.5 V bias under 100 s illuminations. (e) Sensitivity vs time plots of long (ZnO-60) and short (ZnO-10) nanorod photodetectors under long time UV illumination.

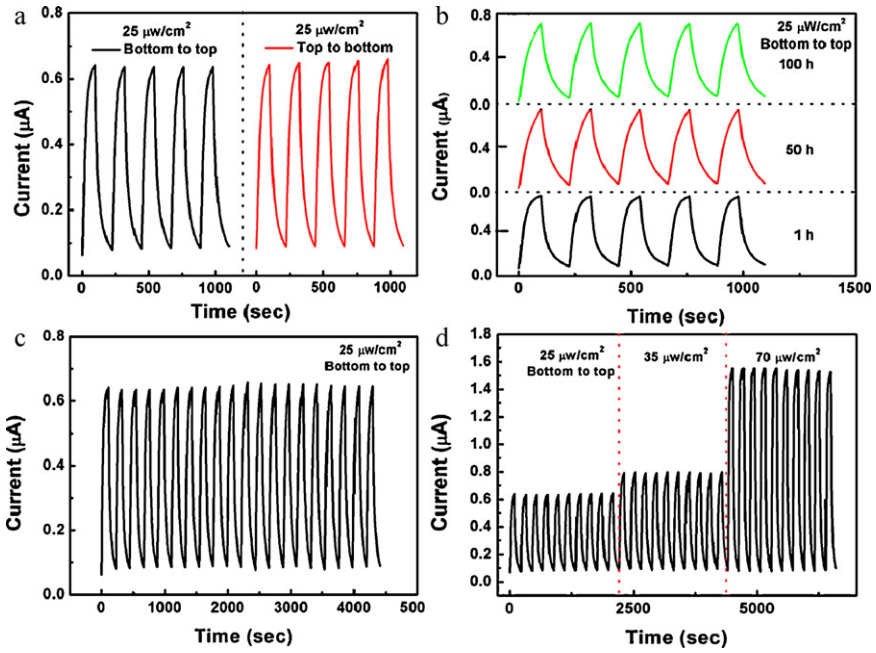

Fig. 7. Stability measurements of ZnO-10/PET photodetector: (a) different orientation UV illumination, (b) retention properties, (c) stability characteristics at 25 μW/cm^2 and (d) multilevel photoresponse performed by various UV power density illuminations.

15 and 25 times higher than the dark current at 0.5 V, respectively. The low dark current is caused by the depletion layer formed near the surface by adsorbed oxygen molecules in the dark environment [$O_{2(g)} + e^- \rightarrow O_2{}^-{}_{(ad)}$]. When the ZnO nanorods are exposed under UV illumination, they generate electron–hole pair [$h\nu \rightarrow e^- + h^+$]. The trapped electrons are released back to the conduction band when the photo-generated holes reacted with the adsorbed oxygen molecules [$h^+ + O_2{}^-{}_{(ad)} \rightarrow O_{2(g)}$], to increase the carrier concentration of the ZnO nanorods [19–21]. Consequently, the current under UV illumination is higher than that in the dark environment.

Fig. 6(b) shows the time-resolved photocurrent of the ZnO-10 nanorods photodetector in response to turn-on and turn-off the UV illumination with power densities of 25, 35 and 70 μW/cm^2, respectively. The photocurrent exponentially increases from 29.2 nA to 1.55 μA within about 100 s and then gradually saturates in the turn-on state with a power density of 70 μW/cm^2. After the UV light was turned-off, the current decreases to 63.2 nA within 120 s. Five cycles of photocurrent switching with various power densities clearly demonstrate the response reproducibility of the ZnO-10 nanorods.

The sensitivity of the UV nanorod photodetector is defined as I_{UV}/I_{Dark}, where I_{UV} is the current of the nanorods in UV turn-on state and I_{Dark} the current of the nanorods in the UV turn-off state. The sensitivity vs time curves under 100 s illumination of the photodetectors are shown in Fig. 6(c), revealing the times of the current recovering to initial values of the ZnO-10, ZnO-20, ZnO-30 and ZnO-60 photodetector are 120, 210, 290 and 470 s, respectively. The ZnO-10 photodetector has faster recovery rate in comparison with other photodetectors. The possible reason is attributed to that the ZnO-10 nanorods have relatively shorter electron transmission length compared to other larger radius nanorods [11,22]. Thus, the photodetector made by the small radius and short ZnO nanorods exhibits shorter recovery time. Fig. 6(d) shows the sensitivity under 100 s illumination of the photodetector as a function of growth time, indicating that the sensitivity increases with an increase of UV light power density and a decrease of growth time. However, under longer time illumination (over 150 s), the long nanorod (ZnO-60) photodetector exhibits higher sensitivity under 25 μW/cm^2 UV density (Fig. 6(e)) because long ZnO-60 provides larger surface area in comparison with ZnO-10.

To further evaluate the photodetector performance of the ZnO-10/PET structure, the orientation, retention, stability and multi-UV intensity characteristics are measured and demonstrated. As shown in Fig. 7(a), the photoresponses are kept the same and without any observable degradation between the measurements of bottom to top and top to bottom UV light illuminations. Fig. 7(b) and (c) depicts the retention and stability characteristics of ZnO-10 photodetector, indicating that the photoresponse can be successively and stably operated more than 100 h (Fig. 7(b)) and the photoresponse at a power density of 25 μW/cm^2 is over 20 cycles, which is more stable and reconstructive in comparison with those at other higher power densities during the cycling measurement. As shown in Fig. 7(d), various UV intensities including 25, 35 and 70 μW/cm^2 are applied to switch the ZnO-10 photodetector into various current states, where the UV illumination is applied form bottom to top. The cycle width used for all measurements is 220 s and the cycle number is 10. Therefore, at least four-level current states can be determined here by controlling the UV power density, which is easily implemented in today's sensor design. Based on the results from Fig. 7(a)–(d), the ZnO-10/PET photodetector has good performance of nondestructive photoresponse, high reliability and multilevel operation under either the illumination at the single UV or different UV power densities. Table 1 summarizes and compares the performance of various ZnO photodetectors. It indicates that our ZnO-10/PET photodetector has the characteristics of faster response and recovery rate under various UV intensity illuminations, higher reliability, excellent orientation properties, multi-level photoresponse in comparison with other reported photodetectors.

4. Conclusions

In this work, we successfully develop a simple method to fabricate high performance ZnO UV photodetector on the flexible PET substrate. Through aqueous solution method, the ZnO nanorods uniformly grow on the PET substrate and the various ZnO nanorods lengths are obtained by adjusting growth time. The

ZnO-10/PET structure reveals good mechanical stability through bending test. Upon UV illumination, the ZnO-10 nanorods photodetector exhibits high sensitivity at low UV power density ($25\,\mu W/cm^2$), fast recovery time (120 s), good orientation properties, reproducible photoresponse (20 cycles) and multi-level operation. The ZnO-10/PET photodetector made by a simple process has high potential for practical applications.

Acknowledgment

This work was supported by the National Science Council of ROC under contract no. NSC 97-2221-E-009-150-MY3.

References

[1] C.Y. Lee, T.Y. Tseng, S.Y. Li, P. Lin, Electrical characterizations of a controllable field emission triode based on low temperature synthesized ZnO nanowires, Nanotechnology 17 (2006) 83–88.
[2] I.C. Yao, P. Lin, T.Y. Tseng, Nanotip fabrication of zinc oxide nanorods and their enhanced field emission properties, Nanotechnology 20 (2009) 125202.
[3] C.Y. Lee, J.Y. Wang, Y. Chou, C.L. Cheng, C.H. Chao, S.C. Shiu, S.C. Hung, J.J. Chao, M.Y. Liu, W.F. Su, Y.F. Chen, White-light electroluminescence from ZnO nanorods/polyfluorene by solution-based growth, Nanotechnology 20 (2009) 425202.
[4] I.C. Yao, P. Lin, T.Y. Tseng, Hydrogen gas sensors using ZnO–SnO_2 core–shell nanostructure, Adv. Sci. Lett. 3 (2010) 548–553.
[5] H.L. Porter, A.L. Cai, J.F. Muth, J. Narayan, Enhanced photoconductivity of ZnO films Co-doped with nitrogen and tellurium, Appl. Phys. Lett. 86 (2005) 211918.
[6] J. Suehiro, N. Nakagawa, S.I. Hidaka, M. Ueda, K. Imasaka, M. Higashihata, T. Okada, M. Hara, Dielectrophortetic fabrication and characterization of a ZnO nanowire-based UV photosensor, Nanotechnology 17 (2006) 2567–2573.
[7] J.B.K. Law, T.L. Thong, Simple fabrication of a ZnO nanowire photodetector with a fast photoresponse time, Appl. Phys. Lett. 88 (2006), 133114-1–3.
[8] H. Kind, H. Yan, B. Messer, M. Law, P. Yang, Nanowire ultraviolet photodetectors and optical switches, Adv. Mater. 14 (2002) 158–160.
[9] H. Huang, Y.C. Lee, O.K. Tan, in: T.Y. Tseng, H.S. Nalwa (Eds.), Handbook of Nanoceramics and Their Based Nanodevices, vol. 5, American Scientific Publishers, Stevenson Ranch, California, 2009 (Chapter 5).
[10] A. Manekkathodi, M.Y. Lu, C.W. Wang, L.J. Chen, Direct growth of alignd zinc oxide nanorods on paper substrates for low-cost flexible electronics, Adv. Mater. 22 (2010) 4059–4063.
[11] Y. Jin, J. Wang, B. Sun, J.C. Blakesley, N.C. Greenham, Solution-processed ultraviolet photodetectors based on colloidal ZnO nanoparticles, Nano Lett. 8 (2008) 1649–1653.
[12] Y.K. Su, S.M. Peng, L.W. Ji, C.Z. Wu, W.B. Cheng, C.H. Liu, Ultraviolet ZnO nanorod photosensors, Langmuir 26 (2010) 603–606.
[13] C.Y. Lee, S.Y. Li, P. Lin, T.Y. Tseng, ZnO nanowires hydrothermally grown on PET polymer substrates and their characteristics, J. Nanosci. Nanotechnol. 5 (2005) 1088–1094.
[14] K. Vanhausden, W.L. Warren, C.H. Seager, D.R. Tallant, J.A. Voigt, B.E. Gnade, Mechanisms behind green photoluminescence in ZnO phosphor powders, J. Appl. Phys. 79 (1996) 7983–7990.
[15] Y.P. Wang, W.I. Lee, T.Y. Tseng, Degradation phenomena of multilayer ZnO–glass varistors studied by deep level transient spectroscopy, Appl. Phys. Lett. 69 (1996) 1807–1809.
[16] S.N. Bai, H.H. Tsai, T.Y. Tseng, Structural and optical properties of Al-doped ZnO nanowires synthesized by hydrothermal method, Thin Solid Films 516 (2007) 155–158.
[17] C.W. Chen, K.H. Chen, C.H. Shen, A. Ganguly, L.C. Chen, J.J. Wu, H.I. Wen, W.F. Pong, Anomalous blueshift in emission spectra of ZnO nanorods with sizes beyond quantum confinement regime, Appl. Phys. Lett. 88 (2006) 241905.
[18] Handbook of Chemistry and Physics, 61st ed., CRC Press, Florida, 1981.
[19] K. Keem, H. Kim, G. Kim, J. Lee, B. Min, K. Cho, M. Sung, S. Kim, Photocurrent in ZnO nanowires grown from Au electrodes, Appl. Phys. Lett. 84 (2004) 4376–4378.
[20] C. Soci, A. Zhang, B. Xiang, S.A. Dayeh, D.P.R. Aplin, J. Park, X.Y. Bao, Y.H. Lo, D. Wang, ZnO nanowire UV photodetectors with high internal gain, Nano Lett. 7 (2007) 1003–1009.
[21] D.H. Wilson, S. Hoyt, J. Janata, K. Booksh, L. Obando, Chemical sensors for portable, handheld field instruments, IEEE Sens. 1 (2001) 256–274.
[22] H. Wang, S. Baek, J. Song, J. Lee, S. Lim, Microstructural and optical characteristics of solution-grown Ga-doped ZnO nanorod arrays, Nanotechnology 19 (2008) 075607.
[23] W. Yen, N. Mechau, H. Hahn, R. Krupke, Ultraviolet photodector arrays assembled by dielectrophoresis of ZnO nanoparticles, Nanotechnology 21 (2010) 115501.
[24] N. Chantarat, Y.W. Chen, S.Y. Chen, C.C. Lin, Enhanced UV photoresponse in nitrogen plasma ZnO nanotubes, Nanotechnology 20 (2009) 395201.
[25] J. Cheng, Y. Zhang, R. Guo, ZnO microtube ultraviolet detectors, J. Cryst. Growth 310 (2008) 57–61.
[26] C.C. Lin, W.H. Lin, Y.Y. Li, Synthesis of ZnO nanowires and their applications as an ultraviolet photodetector, J. Nanosci. Nanotechnol. 9 (2009) 2813–2819.
[27] Y. Li, X. Dong, C. Cheng, X. Zhou, P. Zhang, J. Gao, H. Zhang, Fabrication of ZnO nanorod array-based photodetector with high sensitivity to ultraviolet, Physica B 404 (2009) 4282–4285.
[28] D. Park, K. Yong, Photoconductivity of vertically aligned ZnO nanoneedle array, J. Vac. Sci. Technol. B 26 (2008) 1933–1936.

Biographies

I-Chuan Yao was born in Changhua, Taiwan, in 1983. He received his B.S. degree from the Department of Materials Science and Engineering, National Formosa University, Taiwan in 2005 and M.S. degree from the Institute of Materials Engineering, National Taipei University of Technology, Taiwan in 2007. He is currently working toward the Ph.D. degree at the Institute of Materials Science and Engineering, National Chiao Tung University, Taiwan. His current research interests include ZnO nanostructure, field emission display, and sensor devices.

Tseung-Yuen Tseng received his Ph.D. degree in electroceramics from the School of Materials Engineering, Purdue University, West Lafayette, USA in 1982. He is now a National Endowed Chair Professor in the Department of Electronics Engineering and the Institute of Electronics, National Chiao Tung University, Taiwan. Dr. Tseng's professional interests are electronic ceramics, nanoceramics, ceramic sensors, high-k dielectric films, ferroelectric thin films and their based devices, and resistive switching memory devices.

Pang Lin received his Ph.D. degree from the Department of Materials Science and Engineering, University of California, Los Angeles, USA in 1984. He is a professor in the Department of Materials Science and Engineering, National Chiao Tung University, Taiwan. His current research interests are LTCC microwave ceramics, semiconducting zinc oxide, and energy materials.